Zhang, J. T., Zhang, M., Li, S-X., Pavier, M. J., & Smith, D. J. (2016). Residual stresses created during curing of a polymer matrix composite using a viscoelastic model. Composites Science and Technology, 130, 20-27. DOI: 10.1016/j.compscitech.2016.05.002

Residual stresses created during curing of a polymer matrix composite using a viscoelastic model

J.T. Zhang [a,b*], M. Zhang [a,b], S.X. Li [a,b*], M.J. Pavier [b], D.J. Smith [b]

[a] Department of Engineering Structure and Mechanics, School of Science, Wuhan University of Technology, Wuhan 430070, PR China

[b] Department of Mechanical Engineering, University of Bristol, Bristol BS8 1TR, UK

* Corresponding author. Email: zhjiangtao@whut.edu.cn, lishuxin@whut.edu.cn

Abstract

A modified viscoelastic constitutive model is proposed to predict cure-induced residual stresses in polymer matrix composites. The modifications rely on using the inverse of the Deborah number to describe regimes corresponding to a fully relaxed state, a viscoelastic state and an elastic state. The composite is only in a viscoelastic state for limited ranges of the Deborah number. By considering the evolution of the Deborah number during curing of the AS4/3501-6 composite, the composite is in a fully relaxed state when it is cured at high temperature and the degree of cure is lower than 0.73, and no further changes in the viscoelastic characteristics when the degree of cure is higher than 0.8. A 3D simulation of a composite laminate plate is used to predict the evolution of the residual stresses. The analysis reveals that the accurate simulation on the cure-induced residual stress should include the last two states of the entire cure process, and consider the stress relaxation, thermal deformation and chemical shrinkage.

Keywords: A. Polymer-matrix composites (PMCs), B. Curing, C. Residual stress, C. Stress relaxation, C. Finite element analysis(FEA), Viscoelastic constitutive model

1. Introduction

The creation of residual stress during curing of polymer matrix composites (PMCs) arises because of their inherent anisotropy and inhomogeneity. Their presence can lead to potentially lowering the performance of composite structures, and consequently cure-induced residual stresses should be considered in the design of composite structures. The earliest analyses of residual stresses in PMCs were based on the assumption that PMCs are in the stress-free state at the cure temperature. Therefore residual stresses only develop during the cooling process and can be predicted using elastic models [1, 2]. These traditional elastic models omit the effects of chemical shrinkage, the development of residual stress before cool-down and stress relaxation during the cooling process. These factors are known to have significant effects on the final residual stresses in PMCs [3, 4]. To capture the influence of these factors, a variety of revised cure-dependent elastic models have been proposed [4-7], such as a path dependent constitutive model [4, 5] and the cure-hardening, instantaneous linear elastic (CHILE) model [7]. However, these models, do not consider stress relaxation during the cooling process.

Cure-dependent viscoelastic models have also been developed to predict the development of residual stresses in PMCs. These models recognize that the polymer matrix of PMCs changes from a liquid-like material in the early stages of cure to a viscoelastic solid at the end of curing [8, 9]. Some of the earliest work on the residual stresses in composite materials using a viscoelastic approach was performed by Weitsman [10], although focusing only on the cooling process. White and Hahn [11,

12] developed a process-dependent viscoelastic model to investigate the formation of residual stress in composite laminates during the entire cure cycle. They validated their model through the intermittent cure of non-symmetric cross-ply laminates and measuring process induced residual curvatures. White and Kim [3] introduced a thermo-viscoelastic constitutive equation that depended on the degree of cure and temperature. They then investigated the formation of residual stresses in Hercules AS4/3501-6 composite during an entire cure cycle using a 2D finite element model. Similarly, Lee and Kang [13] performed a thermo-viscoelastic analysis to determine residual stresses in a laminated shell during curing.

More recently, thermo-viscoelastic analyses have been used to explore the development of residual stresses in complex shaped composite structures [14, 15]. However, thermo-viscoelastic properties for PMCs during curing are difficult to be accurately characterized and modeled. Furthermore, the utilization of anisotropic thermo-viscoelastic models leads to long calculation times and requires large amounts of memory to permit storage of the internal state variables [4]. It is therefore necessary to modify the constitutive models or to develop more efficient numerical methods to minimize the computational resources required. Clifford et al, [16] proposed hybrid finite element models containing both shell and solid elements to reduce the required computational resources.

The approach adopted in the present work was to consider whether a cure-dependent viscoelastic model could be modified and to explore methods to achieve this. The model is first introduced in section 2, and based on an analysis of the model, a parameter is

proposed to represent the viscoelasticity of PMCs, and a modified viscoelastic model is proposed. In section 3 the development of viscoelasticity of the Hercules AS4/3501-6 composite during the typical cure cycle is analyzed using data given by White and Kim [3]. In section 4 the application of the modified model is performed and the analysis then applied in section 5 to curing of the Hercules AS4/3501-6 composite. The modified viscoelastic model is compared with predictions using the original viscoelastic model and a cure-dependent elastic model. The effects of stress relaxation, chemical shrinkage and thermal deformation on the development of residual stresses in a $[0/90]_s$ AS4/3501-6 laminate during the entire cure cycle are also analyzed.

2. Viscoelastic constitutive equations

The most general viscoelastic constitutive equation for relaxation of residual stresses generated in composites during curing can be expressed using a hereditary integral, where the stress $\sigma_i(t)$ and mechanical strain $\varepsilon_j(t)$ at any time are given by [13]

$$\sigma_i(t) = \int_{-\infty}^{t} C_{ij}(\alpha, T, t-\tau) \frac{\partial \varepsilon_j(\tau)}{\partial \tau} d\tau \tag{1}$$

$$\varepsilon_j(t) = \tilde{\varepsilon}_j(t) - \beta_j \Delta T - \eta_j \Delta\alpha \tag{2}$$

where α, T and t are the degree of cure, temperature and the current time respectively, C_{ij} is the stiffness matrix, which is dependent on the degree of cure, temperature and time, and the indices i, j = 1-6. $\tilde{\varepsilon}_j$ is the total strain, β_j and η_j are the thermal expansion coefficients (CTE) and chemical shrinkage coefficients (CCE), respectively, ΔT and $\Delta\alpha$ are the changes in temperature and degree of cure, and τ is a dummy variable.

If the material is treated as being thermo-rheologically simple at a constant degree of cure α, and there is no strain history prior to $t = 0$, according to the time-temperature superposition principle, Eq. (1) can be rewritten as [13]

$$\sigma_i(t) = \int_0^{\xi_t} C_{ij}(\alpha, T_r, \xi_t - \xi') \frac{\partial \varepsilon_j(\xi')}{\partial \xi'} d\xi' \tag{3}$$

where T_r is the reference temperature. ξ_t and ξ' are reduced times, given by:

$$\xi_t = \xi(t) = \int_0^t \frac{1}{a_T(\alpha, T)} ds \quad \text{and} \quad \xi' = \xi(\tau) = \int_0^\tau \frac{1}{a_T(\alpha, T)} ds \tag{4}$$

where a_T is a shift factor. For the composite during curing, a_T is functionally dependent on both α and T [13].

In Eq. (3), $C_{ij}(\alpha, T_r, \xi_t - \xi')$ is the stiffness matrix at the reference temperature, and noted as $C_{ij}(\alpha, \xi)$. It can be approximated by the Prony series as [3]:

$$C_{ij}(\alpha, \xi) = C_{ij_\infty} + \sum_{m=1}^{M} C_{ij_m} \exp\left(\frac{-\xi}{\rho_m(\alpha)}\right) \tag{5}$$

where C_{ij_∞} are the fully relaxed stiffnesses, C_{ij_m} are the cure-dependent discrete stiffnesses of elements associated with the $\rho_m(\alpha)$ discrete relaxation times. Substituting Eq. (5) into Eq. (3), the viscoelastic constitutive equation becomes

$$\sigma_i(t) = C_{ij_\infty} \varepsilon_j(t) + \sum_{m=1}^{M} C_{ij_m} \int_0^{\xi_t} \exp\left(-\frac{\xi_t - \xi'}{\rho_m(\alpha)}\right) \frac{\partial \varepsilon_j(\xi')}{\partial \xi'} d\xi' \tag{6}$$

In order to solve the integral in Eq. (6), a recursive algorithm [17] is applied. The integral in Eq. (6) is referred to as $q_{jm}(t)$, and assuming a sufficiently small time increment Δt, the integral $q_{jm}(t)$ can be rewritten as

$$q_{jm}(t) = \int_0^{\xi_{t-\Delta t}} \exp\left(-\frac{\xi_t - \xi'}{\rho_m(\alpha)}\right) \frac{\partial \varepsilon_j(\xi')}{\partial \xi'} d\xi' + \int_{\xi_{t-\Delta t}}^{\xi_t} \exp\left(-\frac{\xi_t - \xi'}{\rho_m(\alpha)}\right) \frac{\partial \varepsilon_j(\xi')}{\partial \xi'} d\xi' \tag{7}$$

where $\xi_t = \xi_{t-\Delta t} + \Delta\xi_t$ and $\Delta\xi_t = \int_{t-\Delta t}^{t} \frac{1}{a_T(\alpha, T)} ds$.

If it is assumed that the degree of cure and temperature are constant during the small time step Δt, and $\varepsilon_j(\xi')$ is a linear function of the reduced time ξ'. Then the two integrals in Eq. (7) can be solved, and a recursive formulation for $q_{jm}(t)$ is given by

$$q_{jm}(t) = A_{1m}(t) q_{jm}(t - \Delta t) + A_{2m}(t) \Delta\varepsilon_j^t \tag{8}$$

where $A_{1m}(t) = \exp(-\frac{\Delta\xi_t}{\rho_m(\alpha_t)})$ and $A_{2m}(t) = \frac{1}{\Delta\xi_t / \rho_m(\alpha_t)}(1 - \exp(-\frac{\Delta\xi_t}{\rho_m(\alpha_t)}))$, α_t is the degree of cure at the current time *t*, $\Delta\varepsilon_j^t$ is the strain increment in time step Δt.

Substituting Eq.(8) into Eq.(6) , the current stress is finally expressed as

$$\sigma_i(t) = C_{ij_\infty} \varepsilon_j(t) + \sum_{m=1}^{M} C_{ij_m} q_{jm}(t) \tag{9}$$

In Eq. (9), the first part represent the contribution of the fully relaxed stiffnesses, and the second part represent the contribution of the discrete stiffnesses to the residual stress. The relaxation behavior of the residual stress contributed by the discrete stiffnesses is controlled by the parameters $A_{1m}(t)$ and $A_{2m}(t)$. It is noticeable that both $A_{1m}(t)$ and $A_{2m}(t)$ are determined by the parameter $\Delta\xi_t / \rho_m(\alpha_t)$. Here we introduce the notation

$$1/De_m = \Delta\xi_t / \rho_m(\alpha_t) \tag{10}$$

These non-dimensional parameters are referred to as the inverse of the Deborah numbers [18], widely used in rheology. If the Deborah number is large the material behaves as a solid, when it is small the material is effectively a fluid.

Both the relaxation parameters $A_{1m}(t)$ and $A_{2m}(t)$ are shown as functions of the inverse of the Deborah numbers in Fig. 1. It can be seen that when $1/De_m > 10^2$, both the values of $A_{1m}(t)$ and $A_{2m}(t)$ approach zero, which indicates the composite is

immediately fully relaxed and the matrix is in a full viscous state (i.e. behaving as a fluid). When $1/De_m < 10^{-2}$, both the values of $A_{1m}(t)$ and $A_{2m}(t)$ approach 1, which indicates the relaxation does not occur in the composite and the matrix is in a glassy state (i.e. behaving as a solid). Only when one or more $1/De_m$ lie between 10^{-2} and 10^{2}, is the composite in a viscoelastic state. In summary, the inverse of the Deborah numbers comprehensively reflect the effects of the degree of cure, the shift factor and the relaxation time on the viscoelasticity of a composite during curing.

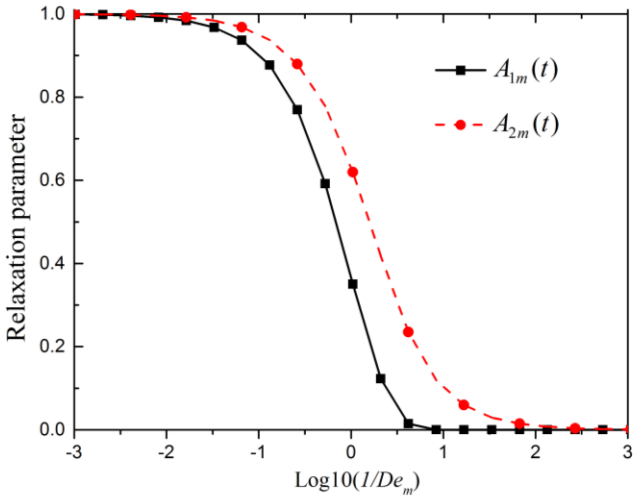

Fig. 1 Variation of relaxation parameters $A_{1m}(t)$ and $A_{2m}(t)$ with the inverse of the Deborah numbers $1/De_m$

By using the development of Deborah numbers during curing, the recursive integral $q_{jm}(t)$ of Eq. (8) can be rewritten as

$$q_{jm}(t)=\begin{cases}0 & Min(1/De_m)>10^{2}\\ A_{1m}(t)q_{jm}(t-\Delta t)+A_{2m}(t)\Delta\varepsilon_j^t & Min(1/De_m)\le 10^{2}\ and\ Max(1/De_m)\ge 10^{-2}\\ q_{jm}(t-\Delta t)+\Delta\varepsilon_j^t & Max(1/De_m)<10^{-2}\end{cases} \quad (11)$$

where $Min(1/De_m)$ and $Max(1/De_m)$ are the minimum and the maximum values of $1/De_m$ $(m=1,2\cdots M)$ respectively.

3. Development of viscoelasticity for Hercules AS4/3501-6 composite during curing

In this work, the behavior of the Hercules AS4/3501-6 composite is used to show how the properties of the composite evolve during curing. The relevant properties of this composite, including the mechanical properties and reaction kinetics were systematically measured and reported by Kim and White [3, 22, 23].

The mechanical properties, thermal expansion and chemical shrinkage coefficients of a fully cured AS4/3501-6 composite are given in Table 1. The fully relaxed stiffness C_{ij_∞} was experimentally determined as being 1/7 the unrelaxed modulus $C_{ij}^u = C_{ij}(\alpha,0)$. The stiffness in the fiber direction C_{11} was assumed to be linear elastic with $C_{11} = C_{11}^u$, while C_{12} and C_{13} were assumed to have the same relaxation times as C_{22} [19, 20].

Table 1 Elastic stiffness $C_{ij}^u = C_{ij}(\alpha,0)$, thermal expansion β_i and chemical shrinkage coefficients η_i of fully cured AS4/3501-6 in the principal material directions [3]

Property	Value	Property	Value
C_{11}^u (GPa)	127.4	$\beta_1(\mu\varepsilon/K)$	0.5
C_{12}^u (GPa)	3.88	$\beta_2 = \beta_3(\mu\varepsilon/K)$	35.3
C_{22}^u (GPa)	10.0	$\eta_1(\mu\varepsilon)$	-167.0
C_{23}^u (GPa)	4.89	$\eta_2 = \eta_3(\mu\varepsilon)$	-8810
C_{66}^u (GPa)	2.57		

The discrete stiffness C_{ij_m} are calculated by [3, 23]

$$C_{ij_m} = (C_{ij}^u - C_{ij_\infty})W_m \Big/ \sum_{m=1}^{9} W_m \tag{12}$$

where W_m is the weight factor. The weight factor W_m and the corresponding relaxation time $\rho_m(\alpha)$ of the AS4/3501-6 composite were determined by White and Kim[3, 23] based on curve fits to the experimental data, and the relaxation times $\rho_m(\alpha)$ is given by

$$\log(\rho_m(\alpha)) = \log(\rho_m(\alpha)) + (f'(\alpha) - (\alpha - \alpha_r)\log(\rho'_m)) \quad (13)$$

where $f'(\alpha) = -0.9464 + 0.0615\alpha + 0.9227\alpha^2$ and $\rho'_m = 10^{9.9} / \rho_m(\alpha_r)$. $\rho_m(\alpha_r)$ is the relaxation time at the reference degree of cure α_r and reference temperature T_r. The values of $\rho_m(\alpha_r)$ and the corresponding weight factors W_m for a AS4/3501-6 composite are listed in Table 2.

Table 2 Relaxation times $\rho_m(\alpha_r)$ and weight factors W_m at the reference degree of cure $\alpha_r = 0.98$ and reference temperature $T_r = 25℃$ for a AS4/3501-6 composite[3]

m	ρ_m(min)	W_m
1	29.2	0.059
2	2.92×10^3	0.066
3	1.82×10^5	0.083
4	1.10×10^7	0.112
5	2.83×10^8	0.154
6	7.94×10^9	0.262
7	1.95×10^{11}	0.184
8	3.32×10^{12}	0.049
9	4.92×10^{14}	0.025

The shift factor $a_T(\alpha, T)$ for AS4/3501-6 composite was defined as [13]

$$a_T(\alpha, T) = 10^{(-1.4\exp(\frac{1}{\alpha-1})-0.0712)(T-T_r)} \quad (14)$$

The reaction kinetics of AS4/3501-6 prepreg have been found to be given by the following empirical equations [24]

$$\frac{d\alpha}{dt} = \begin{cases} (k_1 + k_2\alpha)(1-\alpha)(0.47-\alpha) & \alpha \le 0.3 \\ k_3(1-\alpha) & \alpha > 0.3 \end{cases} \quad (15)$$

The parameters k_i $(i = 1,2,3)$ are defined by Arrhenius rate expressions as

$$k_i = A_i \exp(-\frac{\Delta E_i}{RT}) \quad (i = 1,2,3) \quad (16)$$

where R is the universal gas constant, A_i is a pre-exponential coefficient and ΔE_i is the activation energy. Their values are given in Table 3 [3].

Table 3 Cure kinetic constants for AS4/3501-6 prepreg [3]

Constant	Value	Constant	Value
$A_1(min^{-1})$	2.10×10^9	ΔE_1(J/mol)	8.07×10^4
$A_2(min^{-1})$	-2.01×10^9	ΔE_2(J/mol)	7.78×10^4
$A_3(min^{-1})$	1.96×10^9	ΔE_3(J/mol)	5.66×10^4

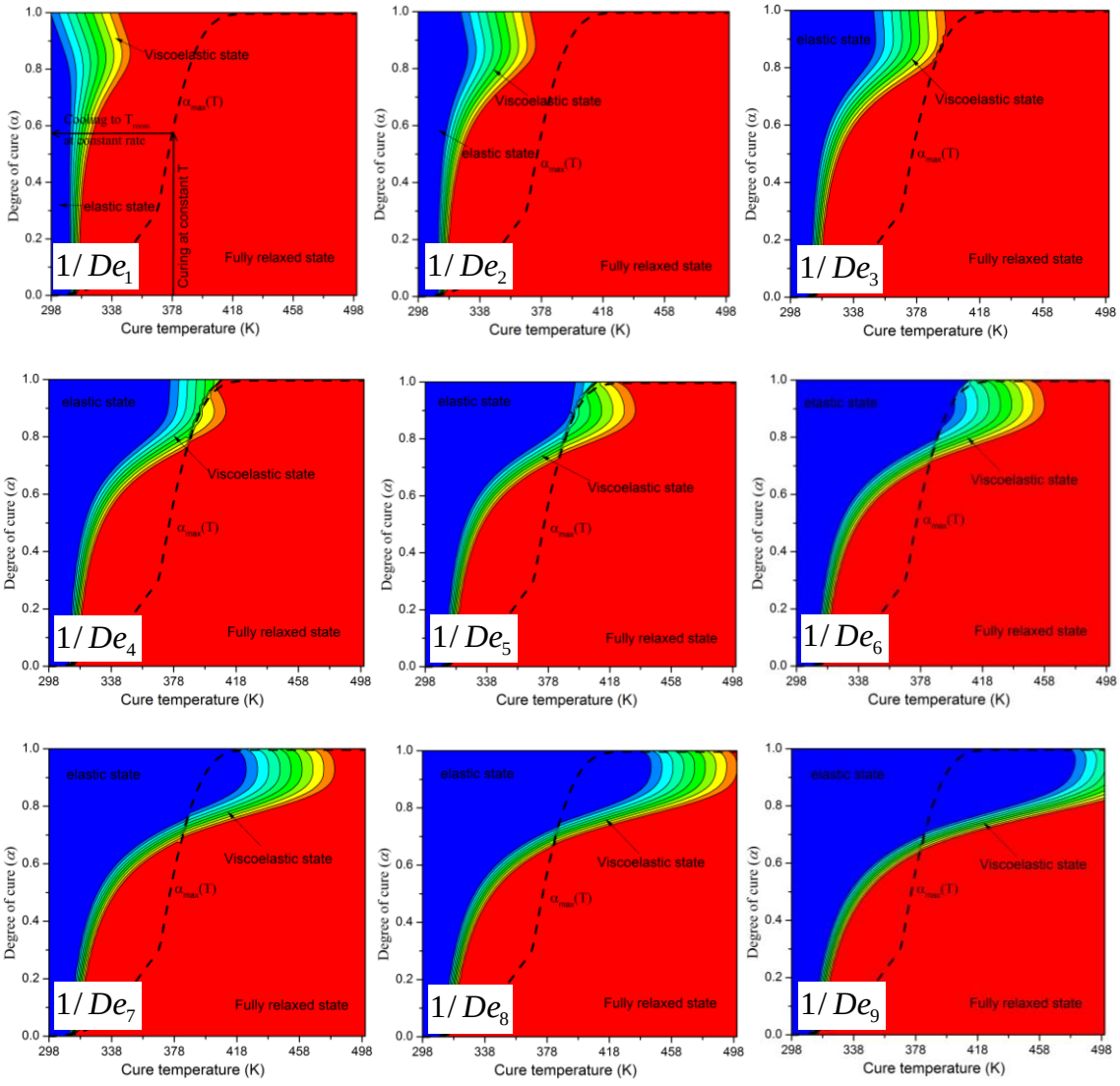

Fig. 2 Contours of the inverse of the Deborah numbers $1/De_m$ for AS4/3501-6 composite ($\alpha_{\max}(T)$ is the maximum degree of cure of composite cured at temperature T_i for 330 min. Red is the fully relaxed state, blue is the elastic state, and the transition between red and blue is the viscoelastic state)

Contours of $1/De_m\,(m=1,2,\cdots,9)$ as functions of α and T were plotted in Fig. 2. The results in Fig. 2 assume that the AS4/3501-6 composite is cured at a constant temperature T_i for 330 minutes, then cooled down to the room temperature (T_{room}) with a constant cooling rate 3K/min. The dashed lines in Fig. 2 represent the maximum degree of cure of the composite when cured at temperature T_i for 330 min. The red region represents the condition that $1/De_m > 10^2$, the m^{th}-term of Eq. (9) is in the fully relaxed state, and it has no contribution to the residual stress. The blue region represents $1/De_m < 10^{-2}$, the m^{th}-term of Eq. (9) is in the elastic state, and the residual stress contributed by this term will be accumulated without relaxation. Only the narrow and belt-like transitional regions between the red and blue regions represent $10^{-2} \le (1/De_m) \le 10^2$, the m^{th}-term of Eq. (9) is in the viscoelastic state, and the stress relaxation takes place for the contributed residual stress at the current curing state. In the following, these belt-like transition regions are referred to as viscoelastic belts.

The results shown in Fig. 2 reveal that the temperature ranges of the viscoelastic belts gradually increase and shift to higher temperatures as curing increases. These tendencies are strengthened by increasing the discrete relaxation time. The maximum temperature range of the viscoelastic belts are achieved at the degree of cure of about 0.8 for all of the discrete relaxation terms. Thereafter they almost no longer increase or shift to higher temperatures by further increasing the degree of cure. This indicates that when the degree of cure attains 0.8, the viscoelastic behavior of the AS4/3501-6 composite does not change with further curing. Therefore the viscoelastic behavior of this composite can be represented by those with degree of cure higher than 0.8.

During curing at 380K or higher temperatures and with the degree of cure less than 0.65, all the discrete relaxation terms are in the fully relaxed state and the degree of cure for the viscoelastic state increases with an increase of the cure temperature. This indicates that when carrying out a residual stress or distortion analysis for the AS4/3501-6 composite cured at 380K or higher temperatures, only the fully relaxed stiffness is required when the degree of cure is less than 0.65, and this value of degree of cure is increased by increasing the cure temperature.

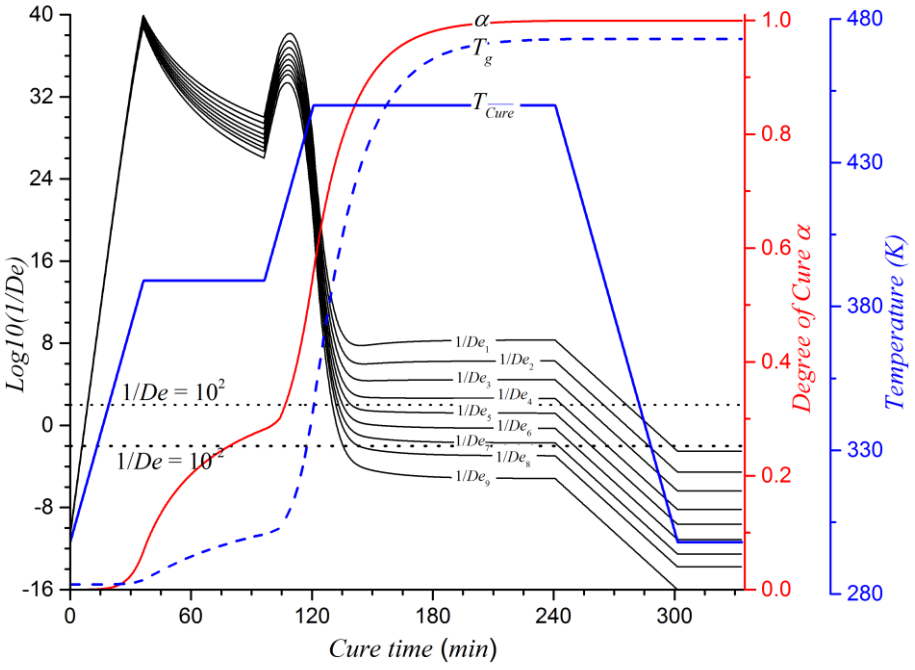

Fig. 3 Cure cycle and the corresponding degree of cure (α), Glass transition temperature (T_g) and the inverse of the Deborah number ($1/De_m$) for the AS4/3501-6 composite during curing

By considering a specific cure cycle, both the degree of cure and the cure temperature are functions of time. The inverse of the Deborah numbers $1/De_m$ are also a function of time. Thus the development of viscoelastic behavior of a composite

during curing can be accurately determined by analyzing the evolution of the inverse of the Deborah number. Results are shown in Fig. 3 for a cure cycle that consists of a 1 hour dwell at 389K followed by a 2 hour dwell at 450K with both heating and cooling rates of 2.5K/minute [3]. The initial temperature was assumed to be $T_0 = 298K$ and the initial degree of cure α_0 was zero. The corresponding degree of cure (α), glass transition temperature (T_g) and the history of the inverse of the Deborah number ($1/De_m$) during curing are also plotted in Fig. 3. The glass transition temperature was calculated using $T_g = 283.34 + 11.86\alpha + 178.04\alpha^2$ [23].

The inverse of the Deborah number ($1/De_m$) increases with increasing cure temperature and decreases with an increase in the degree of cure. At the start of the first heating process, the states of all relaxation terms change quickly into the fully relaxed state, and remain in the fully relaxed state for a long time during the cure process. After the degree of cure attains 0.73 at 130 minutes, the state of the 9th relaxation term changes into a viscoelastic state first. The 9th and 8th relaxation terms become fully elastic at 135 and 143 minutes, respectively. Then they remain in the elastic state in the remainder of the second dwell, with the 5th to the 7th relaxation terms retained in the viscoelastic state in this period. During the cooling process, the 1th to the 7th relaxation terms change gradually from a fully relaxed state or viscoelastic state into a fully elastic state at 298 minutes (306 K).

In summary, the evolution of properties of the AS4/3501-6 composite during curing can be divided into three stages according to the development of the Deborah numbers. The first stage is a fully relaxed state that occurs before 130 minutes, the second stage is

a viscoelastic state occurring before the cooling process, and the last stage is the cooling process after 240 minutes. During the different stages, the composite stiffnesses are very different, leading to different developments of residual stress.

4. Application to finite element models and results

The viscoelastic constitutive Eq. (9) combined with Eqs. (8) and (11), respectively, were implemented in the ABAQUS finite element code through the user subroutine UMAT [21]. A user subroutine UEXPAN in ABAQUS was written to consider the thermal strains and the chemical shrinkage strains.

The finite element simulation on a three-dimensional (3D) cross-ply laminate $[0/90]_s$ was carried out. The model is shown in Fig. 4(a). Due to the symmetry of the geometry, only 1/8th of the model was used as shown in Fig. 4(b). The model was meshed in ABAQUS using 3D brick elements with 8 nodes (element type C3D8). 3200 elements were used with 20 elements in the x_1 and x_2 directions and 8 in the x_3 direction.

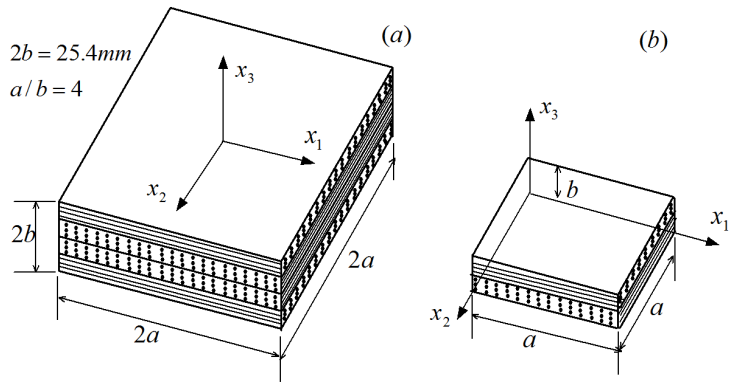

Fig. 4 Geometry model used for residual stress simulation (a) three-dimensional laminate $[0/90]_s$ and (b) $1/8^{th}$ symmetry model

A cure cycle, illustrated in Fig. 3, was then used to investigate the residual stresses created in the AS4/3501-6 laminate composite during curing. The temperature in the

model was assumed to be uniform and varied with the cure cycle. The symmetry boundary conditions were applied to the symmetry planes x=0, y=0 and z=0. A time increment Δt of 15 seconds was used for the calculations.

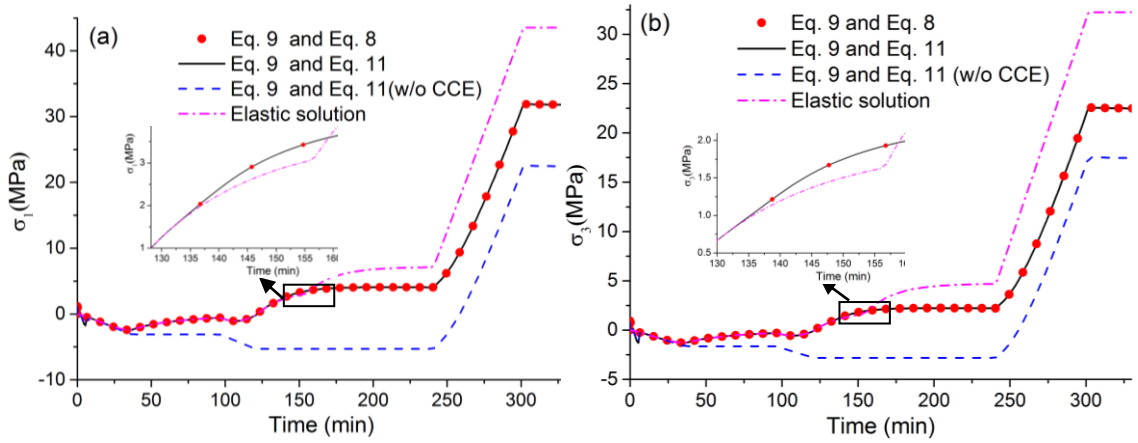

Fig. 5 Comparison of the stress history during curing (a) stress σ_1 at the centre of the model (0,0,0) and (b) interlaminar normal stress σ_3 at (0, a, 0) (w/o CCE indicates that the effects of chemical shrinkage are not calculated)

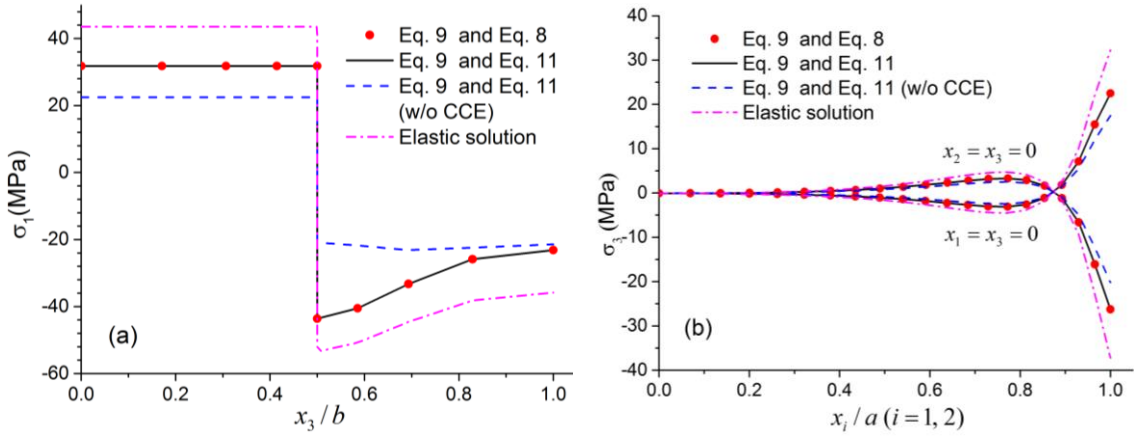

Fig. 6 The distributions of the stress σ_1 at the x_3 axis (a) and the interlaminar normal stress σ_3 at the x_1 and x_2 axes (b) predicted by different models after the entire cure cycle.

The evolution of the residual stress σ_1 at the model center (0, 0, 0) and the interlaminar normal stresses σ_3 at node (0, a, 0) are shown in Fig. 5. The final distributions of the residual stress σ_1 at the x_3 axis and the interlaminar normal stress

σ_3 at the x_1 and x_2 axes are shown in Fig. 6. The results of an elastic model are also shown in Figs. 5 and 6. The elastic results were calculated by assuming the composite was fully relaxed when the cure temperature was higher than the glass transition temperature T_g, and it was unrelaxed if the cure temperature was lower than T_g [25], the elastic solutions were calculated by:

$$\sigma_i(t) = \begin{cases} C_{ij_\infty}\varepsilon_j(t) & T > T_g \\ C_{ij}^u\varepsilon_j(t) & T \le T_g \end{cases} \tag{17}$$

5. Discussion

Examination of the results shown in Figs. 5 and 6 indicates that the predictions using Eq.(11) were the same as those obtained by using Eq. (8) and suggests that introducing the ranges of behaviour in line with the inverse of the Deborah numbers in Eq.(11) were reasonable.

As indicated earlier in section 3, the predictions obtained by the viscoelastic models in the first cure stage (before 130 minutes) were entirely coincident with those obtained using an elastic model as shown in the Fig. 5. This is because during this stage the composite was in a fully relaxed state and only the fully relaxed stiffness C_{ij_∞} was responsible for the development of the residual stress even within the viscoelastic models. Since the fully relaxed stiffness C_{ij_∞} was much lower, and the thermal expansion during heating-up partly compensated for the chemical shrinkage of the composite, the residual stresses developed in this stage were relatively low. For example σ_1 at the centre of the model (0, 0, 0) was only 1.4MPa after 130 minutes. Therefore the end of the first cure stage can be designated as being in a stress free state.

In the initial period of the second cure stage, chemical cure shrinkage caused a

significant increase in the residual stress as shown in Fig. 5. For the viscoelastic models, the 5^{th} to the 9^{th} relaxation terms changed into viscoelastic state and even elastic state, as shown in Fig. 3. These changes in state lead to an increase in composite stiffness. As a result, the residual stresses predicted by the viscoelastic models were higher than those predicted by the elastic model as shown in the inserted figures in Fig. 5, since the fully relaxed stiffnesses were used in the elastic model in this period. The predicted stress difference between the viscoelastic and elastic models becomes obvious after 135 minutes and increases with increasing cure time. This is because the 9^{th} and 8^{th} relaxation terms move into the fully elastic state at 135 and 143 minutes, respectively. Therefore the residual stresses caused by these two terms cannot be relaxed.

As the cure proceeds in the second cure stage, the glass transition temperature T_g attains the cure temperature at 157 minute as shown in Fig. 3. Then the unrelaxed elastic stiffnesses were used in the elastic model. As a result, the residual stresses predicted by the elastic model increase quicker than those predicted by the viscoelastic models as shown in Fig. 5 for the times greater than 157 minutes. The residual stresses predicted by the elastic model continued to increase and the rate of increase in the residual stress slowed during the remainder of the second dwell. This is consistent with the development of the degree of cure in this period. However, for the viscoelastic models, the predicted stresses reach the maximum values at 210 minute, when the composite was almost fully cured (the degree of cure was 0.993). For example, the maximum value of σ_1 at the centre of the plate was about 4.07 MPa at 210 minute. For the remainder of the second dwell, the residual stresses predicted by the viscoelastic models

were almost constant, although the residual stress at the centre did relax very slightly from 4.07 MPa at 210 minute to 4.04 MPa at 240 minute. This was because the 5th to the 7th relaxation terms remained in the viscoelastic state, with the stress relaxation being partly compensated by small amounts of chemical cure shrinkage during this period with the degree of cure being 0.999 at 240 minute.

At the start of the last stage (cooling process) with the 1th to the 7th relaxation terms in a viscoelastic state or becoming viscoelastic from the fully relaxed state, the viscoelastic model exhibited significant nonlinearity due to rapid stress relaxation. As the temperature decreased further, all the relaxation terms gradually moved into an elastic state as shown in Fig. 3, and correspondingly, the relaxation rate also decreased.

Table 4 Comparison of the stresses predicted by different models for σ_1 at the centre of the plate (0,0,0) and σ_3 at the edge center of the plate (0, a, 0)

Model	Present work		2D model [3]		Comments
	σ_1	σ_3	σ_1	σ_3	
Elastic(MPa)	36.4	27.5	37.0	28.9	Cool-down only
	43.5	32.2			Entire cure cycle
Viscoelastic(MPa)	27.7	20.3	29.4	22.6	Cool-down only
	31.8	22.5	32.0	23.8	Entire cure cycle (with CCE)
	22.4	17.5	23.2	19.0	Entire cure cycle (without CCE)

Table 4 lists the final residual stress for σ_1 at the centre of the plate and for σ_3 at an edge center (0, a, 0). The values predicted by White and Kim [3] using a 2D generalized plane strain model are also listed in Table 4 for comparison. Although the evolution of the residual stress during curing and their final distributions predicted by the present 3D model (as illustrated in Figs. 5 and 6) are very close to those predicted

by the 2D model [3]. Their final values predicted by the present 3D model are slightly less than those predicted by the 2D model, and the difference at the plate edge is more obvious comparing with that at the plate centre. This is reasonable since the 2D model implies a strong constraint to make the deformation uniform in the direction normal to the model plane. In the 3D model, the deformation in this direction is free, and the evident distortion happens in the lateral surfaces ($x_2 = a$ and $x_3 = a$). The distortion can partly release the residual stress during curing, and the effect of distortion on the residual stress at the plate edge is more significant than that at the plate centre.

For the present work, the predicted stresses using the viscoelastic models were 27% and 30% lower for σ_1 at (0,0,0) and σ_3 at (0, a, 0) respectively than those predicted by the elastic model for the entire cure cycle. They were 24% and 26% respectively lower for the cool-down process alone. In the viscoelastic models, the same stresses for the entire cure cycle were 14.8% and 10.8% respectively higher than those for cool-down only. When chemical cure shrinkage was not included the residual stresses were underestimated significantly. The predictions without CCE for σ_1 at (0, 0, 0) and σ_3 at (0, a, 0) were 29.6% and 28.6% lower than those with CCE, respectively.

In summary, the final residual stresses were created by a combination of the curing stress (i.e. the residual stress created before cool-down process) and the stresses arising from thermal contraction (i.e. the residual stress formed during cool-down only). Relaxation of the residual stresses should be considered when the composite becomes viscoelastic and can be determined through the Deborah numbers. It is evident that account should be taken of shrinkage from chemical curing.

6. Conclusions

Residual stresses were predicted using a cure-dependent viscoelastic constitutive model within a finite element analysis code. The viscoelastic behaviors were characterized in terms of the inverse of the Deborah numbers $1/De_m$, which comprehensively reflect the effects of the degree of cure, the shift factor and the relaxation time on the viscoelasticity of a composite during curing. When all of the values of $1/De_m$ are higher than 10^2, the composite is in a fully relaxed state. When all of the values of $1/De_m$ are less than 10^{-2}, the composite is in an unrelaxed elastic state. Only when one or more $1/De_m$ lie between 10^{-2} and 10^2, the composite is in viscoelastic state. This classification of states permitted a modified viscoelastic constitutive model to be used to simulate the generation of cure-induced residual stresses.

The temperature and degree of cure conditions for the viscoelastic state of an AS4/3501-6 composite were found to be “belt-like” regions in the temperature and degree of cure plane. The temperature ranges for the viscoelastic belts gradually increase and shift to higher temperatures with increasing cure. The analysis on the viscoelastic behavior of the AS4/3501-6 composite showed that when the degree of cure attains 0.8, there was no further changes in viscoelasticity behavior. In the case of the AS4/3501-6 composite cured under the proposed temperature cycle examined in this paper, its behavior could divided into three stages: a fully relaxed state before 130 minutes, a viscoelastic state before the cooling process, and a cool-down state. The residual stresses developed during the entire cure cycle for a $[0/90]_s$ AS4/3501-6 laminate were calculated using different models. The modified model was verified by

comparing predictions with those created from the original viscoelastic model and a cure-dependent elastic model. The results reveal that the accurate simulation on the cure-induced residual stress should include the last two stages of the entire cure process, and consider the stress relaxation, thermal deformation and also chemical shrinkage.

Acknowledgements

This work was supported through a one year exchange visit to the University of Bristol by Drs M and JT Zhang. Support for their time at Bristol was provided by Wuhan University of Technology and the Fundamental Research Funds for the Central Universities of China under Grant No. 2016IB002. Dr Li is a Visiting Fellow at the University of Bristol. Prof DJ Smith is grateful for the supported provided by the Royal Academy of Engineering, EDF-Energy, Rolls Royce and the University of Bristol.

This paper is dedicated to Prof. Smith who has passed away recently.

References

[1] Hahn HT, Pagano NJ. Curing stress in composite laminates. J Compos Mater 1975; 9:91-105.

[2] Stango RJ, Wang SS. Process-induced residual thermal stresses in advanced fiber-reinforced composite laminates. J Manuf Sci Eng 1984; 106(1):48-54.

[3] White SR, Kim YK. Process-induced residual stress analysis of AS4/3501-6 composite material. Mech Compos Mater Struct 1998; 5:153-186.

[4] Svanberga JM, Holmberg JA. Prediction of shape distortions Part I. FE-implementation of a path dependent constitutive model. Compos Part A 2004; 35:711–721.

[5] Svanberga JM, Holmberg JA. Prediction of shape distortions. Part II. Experimental validation and analysis of boundary conditions. Compos Part A 2004; 35: 723–734.

[6] Bogetti TA, Gillespie Jr JW. Process-induced stress and deformation in thick-section thermoset composite laminates. J Compos Mater 1992; 26: 626-660.

[7] Johnston A, Vaziri R. A plane strain model for process-induced deformation of laminated composite structures. J Compos Mater 2001; 35: 1435–69.

[8] Ruiz E, Trochu F. Thermomechanical properties during cure of glass-polyester RTM composites: Elastic and viscoelastic modeling. J Compos Mater 2005; 39: 881-915.

[9] O'Brien DJ，Mather PT. Viscoelastic properties of an epoxy resin during cure. J Compos Mater 2001; 35(10): 883-904.

[10] Weitsman Y. Optimal cool-down in linear viscoelasticity. J Appl Mech 1980; 47(1):35-39.

[11] White SR, Hahn HT. Process modeling of composite materials: residual stress development during cure. Part I Model Formulation. J Compos Mater 1992; 26(16):2402–22.

[12] White SR, Hahn HT. Process modeling of composite materials: residual stress development during cure. Part II. Experimental validation. J Compos Mater 1992; 26(16):2423–53.

[13] Lee SY, Kang JK. Residual Stresses in a Laminated Shell During Cure. KSME Int J 1999; 13(8):625- 633.

[14]Brauner C, Bauer S, Herrmann AS. Analysing process-induced deformation and stresses using a simulated manufacturing process for composite multispar flaps. J Compos Mater 2015; 49: 387-402.

[15] Li J, Yao XF, Liu YH, Cen ZZ, Kou ZJ, Hu XC, Dai D. Thermo-viscoelastic analysis of the integrated T-shaped composite structures. Compos Sci Technol 2010; 70:1497-1503.

[16] Clifford S, Jansson N, Yu W, Michaud V, Månson JA. Thermoviscoelastic anisotropic analysis of process induced residual stresses and dimensional stability in real polymer matrix composite components. Compos Part A 2006; 37:538–545.

[17] Taylor RL, Pister KS, Goudreau GL. Thermomechanical analysis of viscoelastic solids. Int J Numer Meth Eng 1970; 2:45-59.

[18] Reiner M. The Deborah Number. Physics Today 1964; 17 (1): 62.

[19] Yi S, Chian KS, Hilton HH. Nonlinear viscoelastic finite element analyses of thermosetting polymeric composites during cool-down after curing. J Compos Mater

2002; 36: 3-17.

[20] Kwok K. Mechanics of viscoelastic thin-walled structures. PhD thesis, California Institute of Technology; 2013.

[21] ABAQUS 6.8. Standard user's manual. Hibbitt, Karlsson & Sorensen Inc; 2008.

[22] Kim YK, White SR. Viscoelastic analysis of processing-induced residual stresses in thick composite laminates. Mech Compos Mater Struct 1997; 4:361-387.

[23] Kim YK, White SR. Process-induced stress relaxation analysis of AS4/3501-6 laminate. J Reinf Plast Comp 1997; 16: 2-16.

[24] Lee WI, Loos AC, Springer GS. Heat of Reaction, Degree of Cure, and Viscosity of Hercules 3501 -6 Resin. J Compos Mater 1982; 16:5-10.

[25] Ersoy N, Garstka T, Potter K. Michael R. Wisnom MR, Porter D, Stringer G. Modelling of the spring-in phenomenon in curved parts made of a thermosetting composite. Compos Part A 2010; 41: 410-418.

Figure Captions

Fig. 1 Variation of relaxation parameters $A_{1m}(t)$ and $A_{2m}(t)$ with the inverse of the Deborah numbers $1/De_m$

Fig. 2 Contours of the inverse of the Deborah numbers $1/De_m$ for AS4/3501-6 composite ($\alpha_{\max}(T)$ is the maximum degree of cure of composite cured at temperature T_i for 330 min. Red is the fully relaxed state, blue is the elastic state, and the transition between red and blue is the viscoelastic state)

Fig. 3 Cure cycle and the corresponding degree of cure (α), Glass transition temperature (T_g) and the inverse of the Deborah number ($1/De_m$) for the AS4/3501-6 composite during curing

Fig. 4 Geometry model used for residual stress simulation (a) three-dimensional laminate $[0/90]_s$ and (b) 1/8th symmetry model

Fig. 5 Comparison of the stress history during curing (a) stress σ_1 at the centre of the model (0,0,0) and (b) interlaminar normal stress σ_3 at (0, a, 0) (w/o CCE indicates that the effects of chemical shrinkage are not calculated)

Fig. 6 The distributions of the stress σ_1 at the x_3 axis (a) and the interlaminar normal stress σ_3 at the x_1 and x_2 axes (b) predicted by different models after the entire cure cycle.

Table Captions

Table 1 Elastic stiffness $C_{ij}^u = C_{ij}(\alpha, 0)$, thermal expansion β_i and chemical shrinkage coefficients η_i of fully cured AS4/3501-6 in the principal material directions [3]

Table 2 Relaxation times $\rho_m(\alpha_r)$ and weight factors W_m at reference degree of cure $\alpha_r = 0.98$ and reference temperature $T_r = 25℃$ for a AS4/3501-6 composite[3]

Table 3 Cure kinetic constants for AS4/3501-6 prepreg [3]

Table 4 Comparison of the stresses predicted by different models for σ_1 at the centre of the plate (0,0,0) and σ_3 at the edge center of the plate (0, a, 0)